J|A|C|S
ARTICLES
Published on Web 11/21/2007

The Use of Combinatorial Chemical Vapor Deposition in the Synthesis of $Ti_{3-\delta}O_4N$ with $0.06 < \delta < 0.25$: A Titanium Oxynitride Phase Isostructural to Anosovite

Geoffrey Hyett,[†] Mark A. Green,[‡] and Ivan P. Parkin*[,†]

Contribution from the Christopher Ingold Laboratory, University College London, 20 Gordon Street, London, WC1H 0AJ, United Kingdom, and NIST Center for Neutron Research, National Institute of Standards and Technology, 100 Bureau Drive, Gaithersburg, Maryland 20899-8563

Received May 11, 2007; E-mail: i.p.parkin@ucl.ac.uk

Abstract: We employ, for the first time, a unique combinatorial chemical vapor deposition (CVD) technique to isolate a previously unreported transition-metal mixed-anion phase. The new oxynitride phase, $Ti_{3-\delta}O_4N$ (where $0.06 < \delta < 0.25$), is the first example of a complex titanium oxynitride and was synthesized within composition graduated films formed from atmospheric pressure CVD of $TiCl_4$, NH_3, and ethyl acetate. Characterization was performed by X-ray diffraction, X-ray photoelectron spectroscopy, UV−visible spectra, and SQUID magnetometry. The material crystallizes in the *Cmcm* space group, with the ordered nitrogen ions stabilizing the orthorhombic analogue of the monoclinic anosovite structure, β-Ti_3O_5. The lattice parameters are sensitive to composition, but were determined to be $a = 3.8040(1)$ Å, $b = 9.6486(6)$ Å, and $c = 9.8688(5)$ Å for $Ti_{2.85(2)}O_4N$. Powder samples were prepared through delamination of the thin films for synchrotron X-ray diffraction and magnetic measurements. It is the first example of a new phase to be synthesized using such a combinatorial CVD approach and clearly demonstrates how such techniques can provide access to new materials. This metastable phase with unusual nitrogen geometry has proved to be elusive to conventional solid-state chemistry techniques and highlights the value of the surface growth mechanism present in CVD. Furthermore, the ease and speed of the synthesis technique, combined with rapid routes to characterization, allow for large areas of phase space to be probed effectively. These results may have major implications in the search for new complex mixed-anion phases in the future.

The tendency of nitrides to decompose more readily than oxides as well as to oxidize under atmospheric conditions has historically made synthesis of new nitrides far more difficult than oxides, and consequently they have received much less attention.[1] Despite this relative neglect, nitride phases constitute a significant number of technologically important materials, for example GaInN in blue lasers and LEDs.[2] The relatively high occurrence of useful nitride materials has inspired researchers more recently to refocus on complex ternary and quaternary nitride and oxynitride phases.[3,4] Among these nitrides, there has been particular interest in titanium containing phases, motivated by their importance and wide use as wear resistant and solar control coatings, barrier layers in silicon electronics,[5] and in the case of titanium nitride as a decorative gold-colored coating.[6]

Previous investigations into titanium oxynitrides have uncovered a series of cubic titanium compounds with the rock salt structure and empirical formula TiO_xN_y,[7,8] where the sum of x and y is approximately 1.[9] Materials where the sum of x and y is significantly different to 1 have also been reported. However, in all cases the compound maintains the rock salt structure and accommodates the nonstoichiometry through vacancies on the sublattice sites.[10,11] These TiO_xN_y phases can be considered as a solid solution of titanium(III) nitride, TiN, and the cubic titanium(II) oxide, TiO, with the cubic lattice parameter a of a given TiO_xN_y being found by a Vegard's Law relationship between the value of $a = 4.244$ Å for TiN[12] and $a = 4.172$ Å for TiO.[13] A second type of titanium oxynitride has been extensively reported: the doping of TiO_2 with nitrogen. Research on these materials has been conducted principally to change the band gap of titania and alter its hydrophilic and photocatalytic properties. The extent of this doping is extremely small however, typically less than 0.5 atom % of nitrogen, and

[†] University College London.
[‡] National Institute of Standards and Technology.

(1) Disalvo, F. J. *Science* **1990**, *247*, 649−655.
(2) Nakamura, S. *Semicond. Sci. Technol.* **1999**, *14*, R27−R40.
(3) Niewa, R.; DiSalvo, F. J. *Chem. Mater.* **1998**, *10*, 2733−2752.
(4) Watney, N. S. P.; Gal, Z. A.; Webster, M. D. S.; Clarke, S. J. *Chem. Commun.* **2005**, 4190−4192.
(5) Sherman, A. *J. Electrochem. Soc.* **1990**, *137*, 1892−1897.
(6) Schintlmeister, W.; Pacher, O.; Pfaffinger, K.; Raine, T. *J. Electrochem. Soc.* **1976**, *123*, 924−929.
(7) Drygas, M.; Czosnek, C.; Paine, R. T.; Janik, J. F. *Chem. Mater.* **2006**, *18*, 3122−3129.
(8) Guillot, J.; Chappe, J. M.; Heintz, O.; Martin, N.; Imhoff, L.; Takadoum, J. *Acta Mater.* **2006**, *54*, 3067−3074.
(9) Yang, X. G.; Li, C.; Yang, B. J.; Wang, W.; Qian, Y. T. *Chem. Phys. Lett.* **2004**, *383*, 502−506.
(10) Yang, H.; McCormick, P. G. *J. Mater. Sci.* **1993**, *28*, 5663−5667.
(11) Shin, C. H.; Bugli, G.; Djegamariadassou, G. *J. Solid State Chem.* **1991**, *95*, 145−155.
(12) Bannister, F. A. *Mineral. Mag. J. Mineral. Soc. (1876−1968)* **1941**, *26*, 36−44.
(13) Rostoker, W. *J. Met.* **1952**, *4*, 981−982.

as such are best considered as nitrogen doped materials rather than as true titanium oxynitrides.[14−16]

In contrast to the close-packed cubic TiO_xN_y materials ($d \approx 5.8$ g/cm^3) the new titanium oxynitride presented here is based on nitrogen substitution into the less dense ($d \approx 4.3$ g/cm^3) orthorhombic α-Ti_3O_5 structure, representing what we believe is the first time that anionic substitution has been shown to occur in this material.

The mineral Anosovite was first identified as magnesium-doped Ti_3O_5, an orthorhombic pseudo-brookite phase with lattice parameters $a = 3.747$ Å, $b = 9.465$ Å, and $c = 9.715$ Å, by Rusakov and Zhdanov in 1951.[17] Pure single-crystal studies of Ti_3O_5 have found that at room temperature the structure is actually a related monoclinic cell with lattice parameters $a = 9.752$ Å, $b = 3.802$ Å, $c = 9.442$ Å, and $\beta = 91.55°$,[18] which is known as β-Ti_3O_5. On being heated above room temperature β-Ti_3O_5 undergoes a phase transition between 450 and 460 K (depending on the direction of the transition) to a high-temperature monoclinic phase (β') followed by a further transition above 500 K to the orthorhombic Anosovite structure proposed by Rusakov and Zhdanov,[19] referred to as α-Ti_3O_5. Additionally two more structures are known to be present in the phase diagram below room temperature, known as γ and δ.[20]

The room-temperature monoclinic β-Ti_3O_5 is a semiconductor in which there are three distinct crystallographic titanium sites, each at the center of a distorted TiO_6 octahedron but with evidence of electron localization and metal−metal bonding, similar to the Verwey transition first identified in Fe_3O_4.[21] Bond valance calculations derive valances of these sites as $+3$, $+3^1/_3$ and $+3^2/_3$.[18] The localization of the electron density onto the d^1 Ti^{3+} ions allows metal−metal bonds to form between them, such that the Ti^{3+} ions form "dimers" within the structure with a bond distance of 2.61 Å. The other two crystallographic sites also form a closely associated metal−metal group, a zigzag tetramer of the form $Ti^{+3^1/_3}$−$Ti^{+3^2/_3}$−$Ti^{+3^2/_3}$−$Ti^{+3^1/_3}$ with metal−metal distances of 2.82 Å, 2.77 Å, and 2.82 Å.[18,22] Each group of four titanium ions has two delocalized electrons, which may contribute to a degree of metal−metal bonding within the tetramer.[18] The transformation to the high-temperature α-Ti_3O_5, removes this inequivalency, disrupts the metal−metal bonds, and delocalizes the electrons formerly used in this bonding. The number of distinct titanium crystallographic sites is reduced to two, and metallic behavior is observed showing that the electrons, no longer used for direct metal−metal bonds, become fully delocalized.[22] Bond valance calculations also derive the expected average value of $+3^1/_3$ for both sites,[19] and the shortest Ti−Ti distance increases from 2.61 Å, found in β-Ti_3O_5, to 2.89 Å.

It has been found that cationic substitution into Ti_3O_5 with small amounts of metal ions (as little as 3−6% of the metal content)[23] causes a phase change to the β' polymorph at room temperature. An increase of the dopant metal content to 7−8% or higher[18] destabilizes the monoclinic polymorph completely and the structure converts to the orthorhombic α form at room temperature. This has been demonstrated with an extensive range of metal ions including Sc^{3+}, Cr^{3+}, Li^+, Fe^{3+}, Mg^{2+}, Al^{3+} and V^{3+}.[23−27] This phase transition to the orthorhombic polymorph on cation doping is caused by the destruction of the charge ordered state present in Ti_3O_5 that creates the monoclinic β modification.[23] It can be observed that it is the change in valance that has the principal effect on phase transition by comparing the doping of Mg^{2+} and Li^+ into $M_xTi_{3-x}O_5$. The transition between the β' and α structures occurs with different amounts of substitution for each ion, $x = 0.15$ for Li and $x = 0.3$ for Mg. The titanium oxidation state, however, is the same in both compounds at $+3.47$, that is, this is the threshold value above which insufficient titanium d-electrons remain to stabilize the monoclinic structure.

In this paper, we describe the synthesis $Ti_{3-\delta}O_4N$ (where $0.06 < \delta < 0.25$) as a thin film using combinatorial atmospheric chemical vapor deposition[28] with a triple source of precursors: $TiCl_4$ (metal source), ethyl acetate (oxygen source), and NH_3 (nitrogen source). A number of films were synthesized and the relative ratio of oxygen source to nitrogen source was varied between them to produce films of $Ti_{3-\delta}O_4N$ with differing compositions. The films were investigated by powder X-ray diffraction, X-ray photoelectron spectroscopy, and UV−vis spectroscopy. Delamination of the films provided sufficient powder sample for magnetic measurements as well as Rietveld refinement against synchrotron X-ray diffraction data.

Titanium oxynitrides have been thoroughly investigated by conventional techniques for many years without any indication of this or any other complex (nonrock salt-type) structure. Its identification by combinatorial chemical vapor deposition (CVD)[28] highlights the ability of nonconventional techniques to produce phases that are not accessible by traditional solid-state methods. The possibilities for isolating new complex phases, particularly with mixed-anions, are extensive.

Experimental Section

Film Synthesis. Thin films were synthesized by atmospheric pressure chemical vapor deposition using a cold-walled reactor with the sample being deposited onto standard float glass slides of dimensions 89 mm × 225 mm × 3.2 mm (width, length, thickness). The glass slides were coated on the top surface with a barrier layer of SiO_2 to prevent ions in the glass from migrating into the synthesized film. The CVD reactants were first vaporized in heated bubblers and transported to the reactor by N_2 gas streams. These gas streams entered the reactor through a pair of mixing chambers and a divided baffle manifold that kept the reagents from each mixing chamber separate until the laminar gas flows were inside the reactor. The two separate mixing chambers and reactor entry points are the central design features developed on this apparatus to facilitate combinatorial CVD; using this approach the composition of the reactants is controlled across the film, allowing potential access

(14) Irie, H.; Watanabe, Y.; Hashimoto, K. *J. Phys. Chem. B* **2003**, *107*, 5483−5486.
(15) Borras, A.; Lopez, C.; Rico, V.; Gracia, F.; Gonzalez-Elipe, A. R.; Richter, E.; Battiston, G.; Gerbasi, R.; McSporran, N.; Sauthier, G.; Gyoergy, E.; Figueras, A. *J. Phys. Chem. C* **2007**, *111*, 1801−1808.
(16) Morikawa, T.; Asahi, R.; Ohwaki, T.; Aoki, K.; Taga, Y. *Jpn. J. Appl. Phys., Part 2* **2001**, *40*, L561−L563.
(17) Zhdanov, G. S.; Rusakov, A. A. *Dokl. Akad. Nauk Sssr* **1952**, *82*, 901−904.
(18) Asbrink, S.; Magneli, A. *Acta Crystallogr.* **1959**, *12*, 575−581.
(19) Onoda, M. *J. Solid State Chem.* **1998**, *136*, 67−73.
(20) Hong, S. H.; Asbrink, S. *Acta Crystallogr., Sect. B* **1982**, *38*, 2570−2576.
(21) Walz, F. *J. Phys. Condens. Matter* **2002**, *14*, R285−R340.
(22) Mulay, L. N.; Danley, W. J. *J. Appl. Phys.* **1970**, *41*, 877−879.
(23) Onoda, M.; Ogawa, Y.; Taki, K. *J. Phys. Condens. Matter* **1998**, *10*, 7003−7013.
(24) Kellerman, D. G.; Zhilyaev, V. A.; Perelyaev, V. A.; Shveikin, G. P. *Inorg. Mater.* **1983**, *19*, 221−224.
(25) Grey, I. E.; Li, C.; Madsen, I. C. *J. Solid State Chem.* **1994**, *113*, 62−73.
(26) Grey, I. E.; Ward, J. *J. Solid State Chem.* **1973**, *7*, 300−307.
(27) Steiner, H. J.; Turrillas, X.; Steele, B. C. H. *J. Mater. Chem.* **1992**, *2*, 1249−1256.
(28) Hyett, G.; Green, M.; Parkin, I. P. *J. Am. Chem. Soc.* **2006**, *128*, 12147−12155.

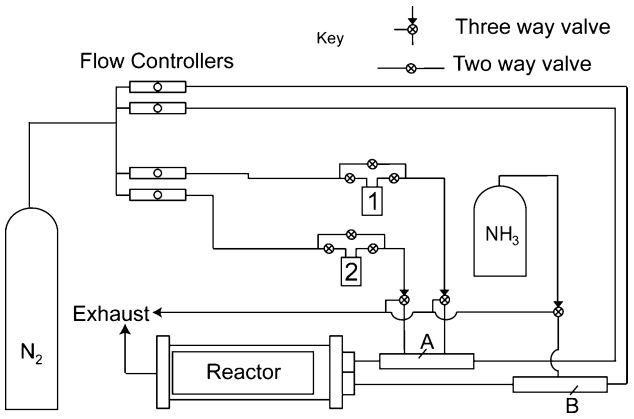

Figure 1. Schematic diagram of the APCVD apparatus, with top down view of the reactor. Of particular importance are the two mixing chambers, with two separate entry points to the reactor, mixing chamber A (on the right) and mixing chamber B (on the left). Left and right in this context are orientated with the forward direction being through the reactor toward the exhaust.

to approximately 1000 products. A schematic diagram of the apparatus is given in Figure 1.

Previous atmospheric pressure CVD work has successfully synthesized TiN phases from $TiCl_4$[29] and NH_3.[30,31] In the work presented here, the Ti−O−N system was formed by addition of ethyl acetate as an oxygen source. In the previous work on titanium nitride it was found that $TiCl_4$ and NH_3 react rapidly in the gas phase to form solid adducts, the most stable of which is $TiCl_4 \cdot 2NH_3$;[32] these can be detrimental to deposition and cause blockages if the vapors are combined too early. The problem of blockage was avoided in this work by introducing $TiCl_4$ and NH_3 into the reactor separately, one through each of the two mixing chambers. The third reagent, ethyl acetate, was introduced through the same mixing chamber as $TiCl_4$; so one mixing chamber (the right-hand one) introduced the $TiCl_4$ and ethyl acetate reagents, and the other mixing chamber (the left-hand one) introduced NH_3 to the reactor. $TiCl_4$ (Aldrich 99.9%) and ethyl acetate (BDH, GPR grade) were volatized in heated bubblers, then transported to the mixing chamber by N_2 (BOC, oxygen free) carrier gas where the $TiCl_4$ and ethlyl acetate streams were combined with each other and a plain line of N_2 as makeup gas. NH_3 (BOC, anhydrous) was transported under its own vapor pressure and also combined in the left-hand mixing chamber with a plain line of N_2. This produced the conditions for the combinatorial aspect of this work, as the oxygen and nitrogen sources entered from opposite sides of the reactor, creating a gradient in the O:N ratio present in the precursor mix horizontally across the substrate and thus a range of deposition conditions in a single experiment.

The use of three precursors provided us with a large number of experimental parameters: temperature, NH_3 flow rate, ethyl acetate flow rate, and $TiCl_4$ flow rate among others; so for simplicity, in the work reported here, all of these parameters were kept at fixed values, and only the ethyl acetate flow rate was varied (Table 1). The $TiCl_4$ and NH_3 flow rates used were kept at approximately 0.1 mol min^{-1}, while the oxygen source (ethyl acetate) flow rate was varied from 0 to 0.0196 mol min^{-1}. Film synthesis was carried out using a deposition time of 60 s, with a substrate temperature of 630 °C.

The novel $Ti_{3-\delta}O_4N$ phase was discovered to form under these conditions with an ethyl acetate flow rate of between 0.0015 and 0.0196 mol min^{-1}, although TiO_2 was noted as a side product at flow of 0.0196 mol min^{-1} of ethyl acetate. In the experiments conducted with an ethyl acetate flow rate of less than 0.0015 mol min^{-1} cubic TiO_xN_y was formed as the dominant phase. Of particular interest among these films, therefore, are those formed with ethyl acetate flow rates of 0.048 and 0.078 mol min^{-1}, where $Ti_{3-\delta}O_4N$ was formed without TiN or TiO_2 as identifiable impurities. In these two reactions the nitrogen/oxygen ratios in the respective precursors were approximately 2:1 and 1:1.

Analytical Methods. X-ray diffraction was carried out on the thin films using a micro-focus Bruker GADDS powder X-ray diffractometer, with a monochromated Cu $K_{\alpha 1+2}$ source, and a CCD area X-ray detector, capable of 0.01° resolution in 2θ. The instrument was used in the glancing incident angle geometry that is best suited to the investigation of thin films; a θ_1 value of 5° was used. The powder sample formed was measured on the ID11 powder diffractometer instrument of the ESRF synchrotron facility using X-ray radiation of wavelength 0.5340 Å, mounted in a glass capillary of 0.5 mm diameter. The recorded diffraction data were modeled using either Le Bail fitting[33] or Rietveld Refinement,[34] both carried out using the GSAS[35] and EXPGUI[36] software suite.

UV−visible transmission and reflection spectroscopy was conducted using a Helios double beam instrument built for compatibility with samples of thin-films on glass substrates. Measurements were standardized relative to a rhodium mirror (reflectance) and blank glass slides (transmission). Absorption, transmission, and reflection spectra were recorded in the range 300−2500 nm.

X-ray photoelectron spectroscopy was conducted using an Escalab 220i-XL instrument with Al Kα radiation. Survey scans were recorded in the range 0−1100 eV (binding energy), and then smaller range, higher resolution scans were recorded of the principal peaks of Ti (2p), O (1s), N (1s), C (1s), and Si (2p). The peaks were modeled using the CasaXPS software system to determine their area, adjusted using sensitivity factors,[37] thus allowing the film composition to be calculated.

Magnetometry measurements were carried out using a Quantum Design MPMS SQUID magnetometer on a 16.3 mg sample of powdered delaminated film, mounted in a gelatin capsule. The magnetization of the sample in different measuring fields was recorded from 0 to 5 T at 298 K. Additionally measurements of the susceptibility against temperature in the range 5−300 K, with the sample cooled both in a field (field cooled, FC) and without a field (zero-field cooled, ZFC) were conducted, using a measuring field of 3 T and then repeated using a measuring field of 4 T. The gradient between the two was used to determine the change in magnetic susceptibility with temperature.

SEM imaging was conducted using a JEOL 6301 field emission instrument, using secondary electron imaging. Samples were mounted side-on and top-down for thickness and morphology investigation, respectively.

Results and Discussion

Films of $Ti_{3-\delta}O_4N$were successfully synthesized from $TiCl_4$, ethyl acetate, and NH_3 precursors. All of the reactant flow parameters were kept constant between experiments, except for the ethyl acetate flow rate which was varied to alter the oxygen to nitrogen precursor ratio. In the two films considered in detail here, the ethyl acetate (oxygen source) flow rate was set such that the N:O ratio in the respective precursors was either 2:1 or 1:1.

Film Formed Using Nitrogen to Oxygen Precursor Ratio of 2:1. The film covered the whole of the substrate but was divided into two sections of different color in transmission: one brown and the other green. The division between these two

(29) Newport, A.; Carmalt, C. J.; Parkin, I. P.; O'Neill, S. A. *J. Mater. Chem.* **2002**, *12*, 1906−1909.
(30) Huang, H. H.; Hon, M. H. *Thin Solid Films* **2002**, *416*, 54−61.
(31) Kurtz, S. R.; Gordon, R. G. *Thin Solid Films* **1986**, *140*, 277−90.
(32) Hojo, J.; Kato, A. *Yogyo Kyokaishi* **1981**, *89*, 277−9.
(33) Lebail, A.; Duroy, H.; Fourquet, J. L. *Mater. Res. Bull.* **1988**, *23*, 447−452.
(34) Rietveld, H. M. *J. Appl. Crystallogr.* **1969**, *2*, 65−71.
(35) Larson, A. C.; Von Dreele, R. B. *Los Alamos Natl. Lab. Rep.* **2000**, 86−748.
(36) Toby, B. H. *J. Appl. Crystallogr.* **2001**, *34*, 210−213.
(37) Wagner, C. D.; Davis, L. E.; Zeller, M. V.; Taylor, J. A.; Raymond, R. H.; Gale, L. H. *Surf. Interface Anal.* **1981**, *3*, 211−225.

Table 1. Details of Reaction Conditions Used to Form Films to Investigate the Ti−O−N System

$TiCl_4$ molar flow mol min^{-1}	NH_3 molar flow mol min^{-1}	ethyl acetate bubbler temp K	ethyl acetate carrier gas flow L min^{-1}	ethyl acetate flow rate mol min^{-1}	composition of the film
0.012	0.018	N/A	0	0	TiN
0.012	0.018	29	0.2	0.0015	TiN and $Ti_{3-\delta}O_4N$
0.012	0.018	34	0.5	0.0048	$Ti_{3-\delta}O_4N$
0.012	0.018	30	1.0	0.0078	$Ti_{3-\delta}O_4N$
0.012	0.018	30	2.5	0.0196	TiO_2 and $Ti_{3-\delta}O_4N$

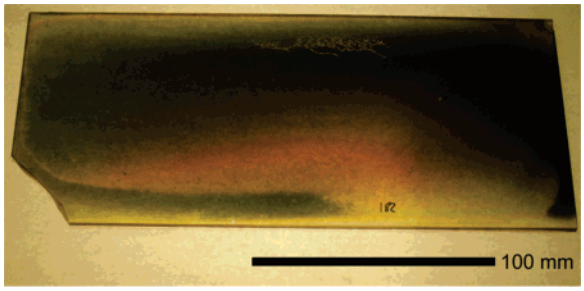

Figure 2. Photograph of the film formed using 0.0048 mol min^{-1} of ethyl acetate, showing the two colored regions, one green and one brown.

sections ran diagonally across the substrate such that each colored section was approximately a right angled triangle, with the brown section having its base along the inlet-edge, nearest to the NH_3 inlet. A photograph of this is shown in Figure 2. All of the films produced were adhesive and stable in air with time.

The colors of the two sections of the film were confirmed by UV−vis spectroscopy, whereby two areas of each of the colored sections of the film were analyzed (these spectra can be seen in the supplementary data). All the spectra show a single very broad asymmetric peak, with a sharp rise at the shorter wavelengths, peaking, and then a trailing edge running into the longer wavelengths. The two spectra recorded from spots of the green section have an $\epsilon_{max} \approx 540$ nm, while the brown sections have an $\epsilon_{max} \approx 615$ nm and a longer tail of transmission at longer wavelengths. Significantly the spectra taken from within the same colored sections of the film, despite coming from different points on the film, have identical spectra. The spectra of the green and brown sections were converted into the *L.a.b.* color coordinate system[38] which found that in transmission the green section has *a*,*b* coordinates of −24.4, 26.43 and the brown section has coordinates of −1.93, 76.75.

The side on SEM measurements conducted on a range of spots in both the green and brown colored sections found that the film thickness was reasonably consistent across the substrate measured as 1300 nm in the green section, and 1000 nm in the brown section, for this deposition of 1 min. The top-down SEM images revealed a similarly consistent morphology for both colored sections of the film, reminiscent of fused platelets. Figure 3 shows an example SEM image of the film morphology.

To determine the composition of the film XPS analysis was conducted on two sections of the film, one from the brown section and one from the green section (Table 2). Peak positions were calibrated relative to an adventitious trace surface carbon impurity taken to be at 284.6 eV. This found that both sections of the film contained Ti, O, and N. In the brown section of the film the O 1s peak was found at 530.1 eV and the N 1s at 395.9

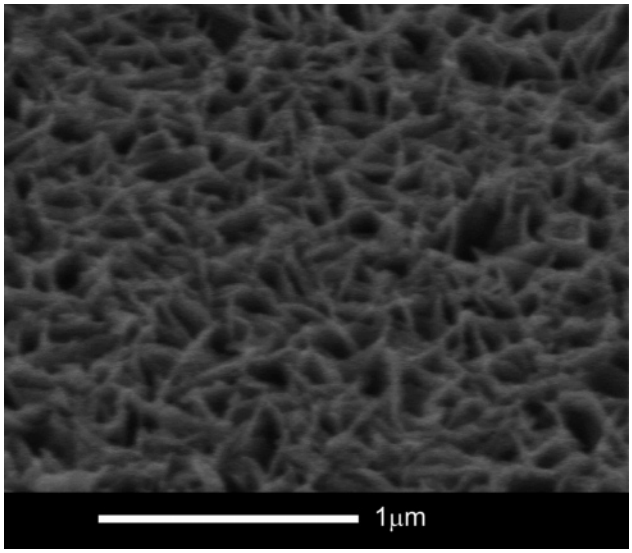

Figure 3. SEM image showing the unusual "fused platelet" morphology found in all of the films of $Ti_{3-\delta}O_4N$.

Table 2. Values for the Binding Energies of the Ti 2p3/2, O 1s, and N 1s Peaks Found in the X-ray Photoelectron Spectra of the Green and Brown Sections of the First Film, with an N:O Precursor Ratio of 2:1[a]

	peak position in binding energy		
compound	Ti 2p3/2 (eV)	O 1s (eV)	N 1s (eV)
green section of film	458.0	530.0	395.8
brown section of film	457.9	530.1	395.9
TiO_2	458.6	530.0	N/A
TiN	455.1	N/A	397.1
TiO_xN_y	456.5	unknown	396.0

[a] The values found in TiO_2, TiN, and TiO_xN_y are also given, for comparison.

eV, values consistent with the database values for O^{2-} and N^{3-} ions bound to titanium of 530.0 eV for TiO_2 and 397.1 eV for TiN. Compounds with nitrogen in oxidation state 0 or higher have values of over 400 eV, so the value of 395.9 eV observed strongly suggests anionic nitrogen is present. A single titanium 2p3/2 peak was found at 457.9 eV, again consistent with the determination of the compound as titanium oxynitride, being intermediate for the values found for TiO_2 (458.6 eV) and TiN (455.1 eV). The titanium peak has been reported at 456.5 eV in cubic titanium oxynitride.[39] In the green section of the film similar peak positions were found: 395.8 eV for N 1s, 530.0 eV for O 1s, and 458.0 eV for Ti 2p3/2. The peak positions then are all consistent with the hypothesis that all three elements are present in the same phase, a titanium oxynitride. Compositional analysis from the XPS found the brown section to be composed of 37.1 atom % Ti, 50.5 atom % O, and 12.4 atom

(38) Palgrave, R. G.; Parkin, I. P. *J. Am. Chem. Soc.* **2006**, *128*, 1587−1597.

(39) Lu, F. H.; Chen, H. Y. *Thin Solid Films* **1999**, *356*, 374−379.

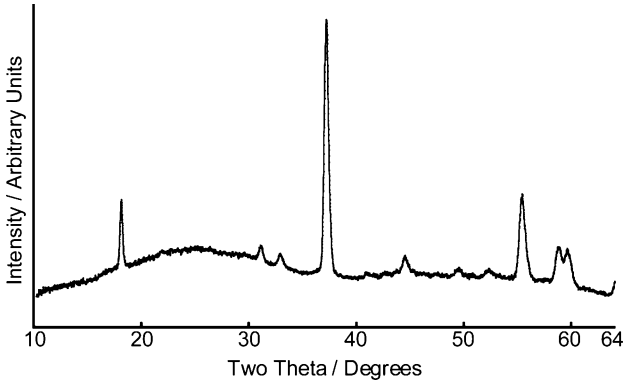

Figure 4. Diffraction pattern of thin film of $Ti_{3-\delta}O_4N$ recorded on GADDS diffractometer. The broad feature present in the background is caused by diffraction from the amorphous glass substrate.

% N. The green section located on the diagonal strip further from the NH_3 inlet contained 36.0 atom % Ti, 51.2 atom % O, and 12.8 atom % N. Inspection of the survey scans (0−1100 eV) taken of both sections of the slide found only peaks that could be identified as belonging to C, Ti, O, or N. No other peaks, and hence no other elements, could be identified. An attempt was made to perform an additional quantitative analysis on the sample using wavelength dispersive X-ray analysis on an SEM instrument. This confirmed that the only detectable elements present were Ti, O, and N, but a quantitative analysis was not possible owing to the overlap of the Ti and N peaks.

X-ray diffraction patterns recorded on both the green and brown sections of film could not be exactly matched to any known titanium containing phase. The closest match to the diffraction pattern of a titanium compound that could be made was to that of the high-temperature, orthorhombic phase of α-Ti_3O_5, but with a peak mismatch between the database and recorded pattern, suggestive of a shift in the lattice parameters. The diffraction pattern is shown in Figure 4. Indexing the peaks in the *Cmcm* space group of α-Ti_3O_5 gave a model that fits all of the observed peaks but with a significant number of the predicted peaks absent in the recorded pattern because of preferred orientation, a common observation in thin films.[40,41] Because of these limitations Le Bail fitting[33] was used to determine the lattice parameters that best fitted the observed diffraction peaks, conducted in the *Cmcm* space group of Anosovite. This refinement found that the parameters of the green section were $a = 3.781(1)$ Å, $b = 9.697(1)$ Å, and $c = 9.901(1)$ Å, with a unit cell volume of 363.1(1) Å,^{3} while the brown section had parameters $a = 3.804(1)$ Å, $b = 9.705(2)$ Å, and $c = 9.903(1)$ Å, with a unit cell volume of 365.5(1) Å.^{3} These cell volumes compare to 350 Å^3 found in the pure monoclinic Ti_3O_5. Similarly high unit cell volume values of 365−370 Å^3 are, however, found in the cationically substituted $Mg_xTi_{3-x}O_5$ ($0.3 < x < 0.9$)[27] and $Li_xTi_{3-x}O_5$ ($0.05 < x < 0.5$).[23] Inadvertent metal doping, however, cannot explain the properties observed in the films prepared in this work as the XPS and WDX study has revealed that no metal ions other than titanium are present, within the 0.1 atom % detection limit, in the necessary amounts (ca. 7 atom %) to stabilize the orthorhombic phase.

The results of the diffraction strongly suggest that a new phase has been synthesized, with a structure analogous to high-temperature orthorhombic α-Ti_3O_5 ($TiO_{1.67}$), but with nitrogen insertion, as determined by the presence of nitrogen peaks in the XPS, with a binding energy associated with titanium nitrides and oxynitrides and the change in lattice parameters observed from the indexing of the diffraction patterns. The XPS compositional results gave anion/metal ratios of 1.70 and 1.78 for the brown and green sections, respectively, compared to the expected 1.67 based on this Ti_3X_5 model, so there is an excess of anions. This can be interpreted as extra-anion intercalation with a fully occupied metal sublattice, or as a normally occupied anionic sublattice, with vacancies on the metal sublattice accounting for the higher ratio. The lack of suitable sites in the structure for anion intercalation, and indeed further evidence from X-ray diffraction (that will be discussed later, in regard to the powder samples of oxy-nitride), effectively precluded the occupation of intercalation sites. Such titanium sublattice vacancies have previously been observed in cationic-doped $Mg_{0.24}Ti_{2.66}O_5$[25] and also in the nitride $Ti_{0.76}N$,[42] so it is reasonable to suggest that a similar titanium deficiency occurs in $Ti_{3-\delta}O_4N$. This yields a formula of $Ti_{2.94}O_{4.00}N_{1.00}$ for the brown section and $Ti_{2.81}O_{4.00}N_{1.00}$ for the green section, with O/N ratios of 4:1 in both sections. The variation in titanium content gives the two different sections different titanium oxidation states of +3.7 for the brown section and of +3.9 for the green section. These values are above the threshold oxidation state of +3.47 for stability of the monoclinic Ti_3O_5 structure and explain why the orthorhombic structure is observed.

The sheet conductivity of the films was measured, and the experiments found that the green sections of film had sheet resistivity of 300−500 ohms/square, while the brown sections had values of 5000−6000 ohms/square. This is a significant difference in the sheet resistance between the two sections, which may be due to fundamental differences in conductivity between them, but sheet resistance is not simply dependent on the electronic properties of the material but also heavily influenced by such factors as film thickness and surface morphology. Given the similarities in structure and oxidation state, as implied from the diffraction and XPS measurements, it seems likely that the increased thickness of the green section (1300 nm vs 1000 nm) leads to a relative reduction in its resistance. Differences in morphology may also be playing a critical role.

Film Formed Using a Nitrogen to Oxygen Precursor Ratio of 1:1. In a second set of films the ethyl acetate reactant flow was increased to 0.0078 mol min^{-1}, while the NH_3 and $TiCl_4$ flow rates were maintained at the same levels as in the previous film, thus giving a O:N precursor ratio of 1:1. Visual inspection of the film formed under these conditions found that it was green in color across the whole substrate, with no brown section. A UV−vis spectrum recorded on this film shows that it was identical to that recorded on the green section of the first film. Side-on SEM imaging again gave a thickness of 1300 nm, grown in 1 min.

The X-ray diffraction pattern recorded on the film synthesized with the higher ethyl acetate content could also be indexed using a similar cell as the patterns recorded on the two-colored film; a Le Bail fitting in the *Cmcm* group gave lattice parameters of

(40) Blackman, C. S.; Parkin, I. P. *Chem. Mater.* **2005**, *17*, 1583−1590.
(41) Hyett, G.; Blackman, C. S.; Parkin, I. P. *Faraday Discuss.* **2007**, *136*, 329−343.
(42) Christensen, A. N. *Acta Chem. Scand., Ser. A* **1975**, *29*, 563−564.

Table 3. Analysis of the Films' Composition Based on XPS Results

ethyl acetate flow rate used in synthesis mol min^{-1}	color	composition atom % Ti	O	N	formula	O:N ratio
0.0048	green	36.0	51.2	12.8	$Ti_{2.81}O_{4.00}N_{1.00}$	4.0
0.0048	brown	37.0	50.5	12.4	$Ti_{2.94}O_{4.01}N_{-0.99}$	4.1
0.0078	green	35.4	53.0	11.6	$Ti_{2.75}O_{4.10}N_{0.90}$	4.58

a = 3.813(1) Å, b = 9.651(1) Å, c = 9.917(1) Å, and a corresponding unit cell volume of 364.8(1) Å^3. Preferred orientation was also observed in the pattern of this second film preventing structural refinement being conducted.

The XPS analysis conducted on this second film gave the composition, assuming anionic substitution, as $Ti_{2.75}O_{4.10}N_{0.90}$ (35.4 atom % Ti, 53.0 atom % O, and 11.6 atom % N), with an O/N ratio of 4.58. This composition has a slightly higher O:N ratio than the green section of the previously discussed film, as would be expected given the change in precursor ratio, but this change in O:N ratio does not seem to have a significant effect on either the lattice parameters or the UV−vis spectroscopic properties. Instead the film color seems to be dependent on the oxidation state of the titanium ion, which in the green sections lies between +3.91 and +3.96, while the brown section of the first film has a lower oxidation state of +3.7. The XPS results from all the analyzed sections of both films are summarized in Table 3.

Analysis of the Powder Sample. In terms of the materials structure, the recurrent problem in both of the discussed films was that effective structural refinement could not be carried out using the diffraction data recorded on them, owing to the presence of a large degree of preferred orientation. This problem was overcome by a further experiment using the higher ethyl acetate precursor conditions (0.0078 mol min^{-1}), but with an increased deposition time of 120 s. Under these conditions the film delaminated, and the flakes of this delaminated film were collected and ground, yielding ca. 15 mg of polycrystalline powder. Diffraction data were recorded of the powder on the high-intensity ID11 X-ray powder diffractometer at the ESRF synchrotron facility.

The initial model used in the Rietveld refinement using the diffraction data recorded on the powder was that of the high-temperature α-Ti_3O_5[17] but with the lattice parameters changed to match those determined from the previous Le Bail refinement of the thin-film samples of $Ti_{3-\delta}O_4N$ giving a cell volume of approximately 365 Å^3 compared to approximately 345 Å.^{3} The atomic position, lattice, peak profile, and background parameters of this pseudo-α-Ti_3O_5 model were then allowed to refine, but the atomic displacement parameters of all of the atoms were fixed at 0.005 Å.^{2} This first approximation of the structural model provided a reasonably good fit to the data, with agreement factors of χ^2 = 2.43, wR_p = 5.1%, and R_F^2 = 6.4%. This evidence supports the supposition that the nitrogen in the structure is located on the oxygen sites of the Anosovite structure and not entering new intercalation sties. If this were the case it is unlikely that such a good fit would be found between the Anosovite derived model and the data; excess electron density off the oxygen sites would lead to a significantly different pattern.

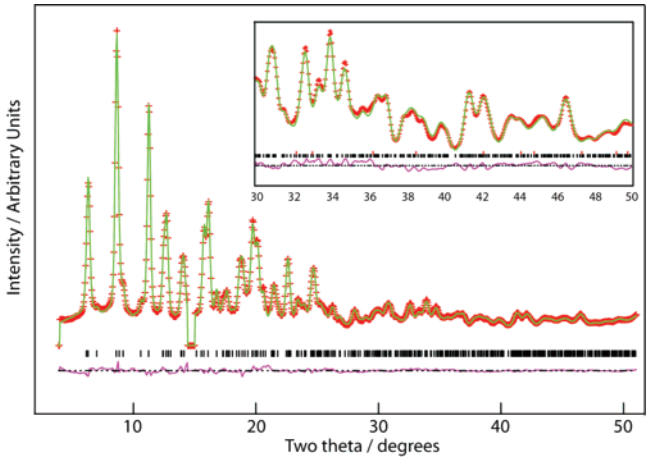

Figure 5. Rietveld refinement of the Anosivite *Cmcm* structural model against diffraction data recorded on powdered delaminate sample of $Ti_{2.85}O_4N$, recorded on ID11 at the ESRF synchrotron facility. Data is shown in red, model in green, and difference plot in purple. The black tick marks under the pattern indicate the position of indexed peaks of $Ti_{2.73}O_4N$. Inset shows an enlarged image of the pattern from 30° to 50° 2θ.

The nitrogen was initially inserted into the structural model onto the same sites as the oxygen atoms. The atomic occupation factors were set such that each anion site was 20% nitrogen and 80% oxygen, matching the O/N ratio determined from the XPS analysis. The isotropic displacement parameters of the anions were also all constrained to be equal to each other. Additionally it was found that the displacement parameters of the two titanium ion sites had to be fixed at 0.001 Å^2, to prevent them becoming unphysical. Further examination of the diffraction pattern also identified the presence of a weak extra peak at approximately 14.6° 2θ. The position of the peak was within the range available to the principal peak of the cubic TiO_xN_y phases (a = 4.172−4.244 Å), and given the nature of the sample it seems most likely that this is the origin of the peak. However, as the peak is very weak and observed only as a barely detectable shoulder, and as no other peaks could found to confirm the phase identification, the shoulder was excluded from the refinement. This nitrogen containing model significantly improved the fit achieved with the goodness of fit parameters dropping to χ^2 = 1.100, wR_p = 3.73%, and R_F^2 = 4.05%.

An additional analysis was then undertaken whereby the relative O/N ratio of each anion site was allowed to vary. These additional degrees of freedom strongly shifted the ratio of the two 8*f* sites to favor oxygen, and the 4*c* to favor nitrogen. On the basis of this a second model was derived such that the 8-fold sites were solely occupied by oxygen, whereby the 4-fold site contained nitrogen exclusively, which maintains the overall 4:1 ratio of oxygen to nitrogen observed from XPS. Additionally a model was derived using only oxygen on the anion sites, for comparative purposes. The random anion occupancy model gave a χ^2 = 1.100, compared with the ordered nitrogen model of χ^2 = 0.9454. The oxygen only model gave a value of χ^2 = 1.146. From these results it is clear that the nitrogen is ordered onto the *4c* site. Figure 5 shows the diffraction pattern, and the refined model pattern fitted to it; Figure 6 shows the unit cell of the structural model.

The full structural details of the model are given in Table 4, the derived structural formula is $Ti_{2.85(2)}O_4N$ and the titanium oxidation state is +3.86. The volume of approximately 362 Å^3 is significantly larger than the undoped monoclinic β-Ti_3O_5 with

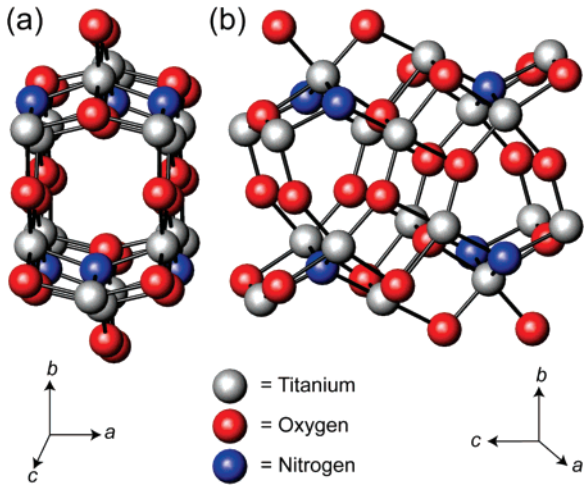

Figure 6. Representation of the unit cell of the $Ti_{2.85}O_4N$ model. Grey atoms are titanium, red is oxygen, and blue is nitrogen: (a) view of the 001 face; (b) view of the 100 face.

Table 4. Structural Parameters of the $Ti_{2.85(2)}O_4N$ Model[a]

atom site	Wyckoff position	*x*	*y*	*z*	U_{iso} (Å^2)	fractional occupancy
Ti1	4*c*	0	0.6956(2)	0.25	0.001	0.933(6)
Ti2	8*f*	0	0.6392(1)	0.5663(1)	0.001	0.958(5)
O1	8*f*	0	0.1861(4)	0.5715(4)	0.005(1)	1.0
O2	8*f*	0	0.5470(5)	0.3825(3)	0.005(1)	1.0
N3	4*c*	0	0.7341(6)	0.75	0.005(1)	1.0

[a] *Cmcm* space group with $a = 3.8040(1)$ Å, $b = 9.6486(6)$ Å, $c = 9.8688(5)$ Å and volume = 362.21(2) Å^3; $\chi^2 = 0.9454$, $wR_p = 3.21\%$, and $R_F^2 = 3.9\%$ for 49 variables recorded at 295 K.

a unit cell volume of 349.7 Å.^{3} The expansion of the unit cell caused by the nitrogen doping cannot be explained on the basis of changes in the titanium−anion bond length, as the average bond length in both β-Ti_3O_5 and $Ti_{2.85(2)}O_4N$ is 2.02(1) Å. Instead the principle reason for the expansion is the breaking of the titanium−titanium bonds present in β-Ti_3O_5, where the shortest metal−metal distance is 2.61 Å. In $Ti_{2.85(2)}O_4N$ the shortest metal−metal distance has been increased to 2.99 Å; the presence of nitrogen increases the formal oxidation state of the Ti to near +3.86, above the threshold of +3.47 where the metal−metal bonding that stabilizes the monoclinic form is disrupted. Comparison with the Li^+ and Mg^{2+} metal-doped Ti_3O_5 with similarly high-titanium oxidation states, those of $Li_{0.5}$-$Ti_{2.5}O_5$ and $MgTi_2O_5$, also show this increase in cell volume compared to the undoped β form with values of 367.3 Å^3 and 364.73 Å^3, respectively. These are slightly larger than the increase found for $Ti_{2.85(2)}O_4N$ as the metal-doped examples have the disruption of the metal−metal bonds and additionally the presence of the larger Li^+ and Mg^{2+} ions to increase the unit cell dimensions further.

In $Ti_{2.85(2)}O_4N$ both titanium sites are in 6-fold coordination to the anions, in distorted octahedra. Ti1 has a coordination sphere of five oxygen ions and one nitrogen ion, while the Ti2 site has four oxygen ions and two nitrogen ions. The coordination environment of each Ti site is shown in Figure 7, where the extent of this distortion can be observed with individual Ti−N or Ti−O bond lengths varying from 1.861(4) to 2.159(4) Å (Table 5). The range of anion environments within the structure is even greater. The O1 and N3 sites are four coordinate

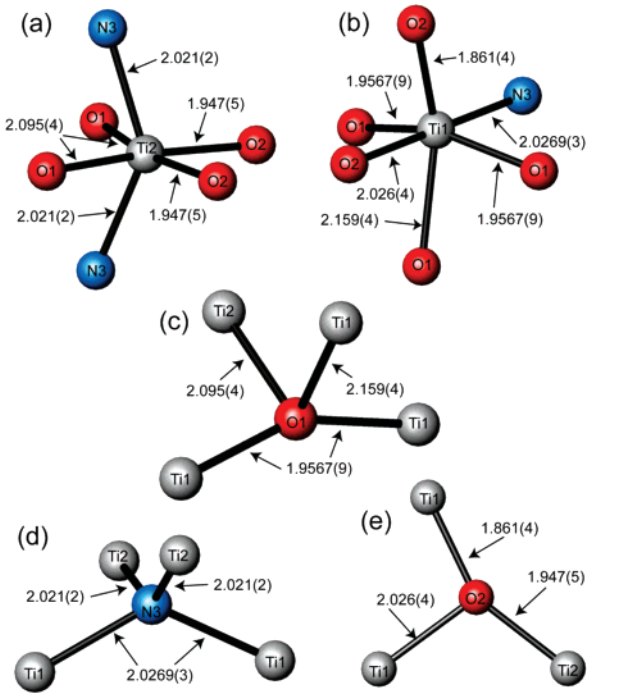

Figure 7. Representation of the coordination environment of the ions in the structure, with bond lengths marked in Å: (a) Ti2, (b) Ti1, (c) O1, (d) N3, and (e) O2.

Table 5. Ti−O and Ti−N Bond Lengths for Each of the Titanium Environments Found in the Structure of $Ti_{2.85(2)}O_4N$

Ti1 environment	bond length (Å)
Ti1−O1 (×2)	1.9567(9)
Ti1−O1	2.159(4)
Ti1−O2	2.026(4)
Ti1−O2	1.861(4)
Ti1 − N3	2.0269(3)
Ti2 environment	**bond length (Å)**
Ti2−O1 (×2)	2.095(4)
Ti2−O2 (×2)	1.947(5)
Ti2−N3 (×2)	2.021(2)

to titanium in distorted tetrahedral environments, while the O2 site is in three coordination. These environments are also shown in Figure 7.

The magnetic properties of a sample of $Ti_{2.85(2)}O_4N$ were investigated using SQUID magnetometry on a 16.3 mg sample of the powder by measuring the magnetization against both field and temperature. Inspection of the magnetization against field measurements found that the response was linear above 1.5 T (where small ferromagnetic impurities had been saturated). The variation in the magnetic susceptibility with temperature was found by taking the gradient of the magnetization between measuring fields of 3T and 4T and is plotted in Figure 8. This shows that the sample has an extremely small susceptibility, consistent with the small number of d-electrons available per titanium ion (0.14 e^- per Ti), and no features in the variation of temperature indicative of either ferromagnetic or antiferromagnetic behavior. A plot of the inverse susceptibility against temperature gives a nonlinear plot (also Figure 8), showing that in this temperature range the material is not in the Curie−Weiss regime.

It is interesting to note that over 1000 papers have been published on the cubic titanium oxynitride, over 300 on the

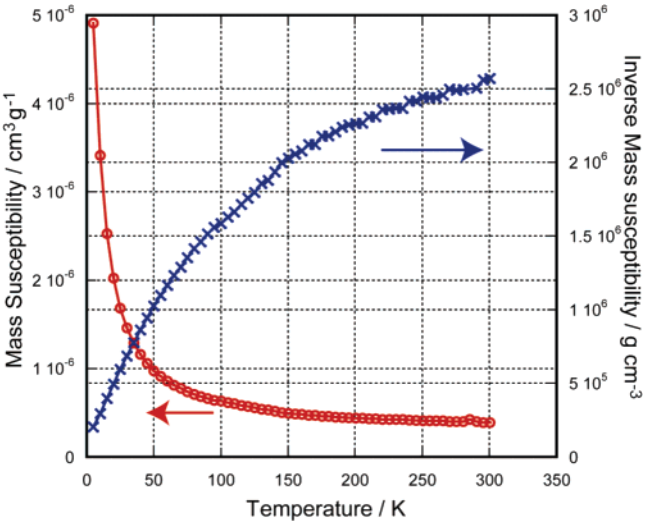

Figure 8. Plot of $Ti_{2.85}O_4N$ mass susceptibility against temperature (red plot, empty circles, *y*-axis to left) and of the inverse mass susceptibility (blue plot, filled circles, *y*-axis to the right).

nitrogen doping of TiO_2 (based on a search of the chemical abstracts of titanium oxynitride and nitrogen-doped TiO_2, respectively). So the titanium−oxygen−nitrogen system is one that has been extensively investigated over a number of years. So the appearance of a previously unreported, room-temperature phase, with a structure significantly different to any currently reported titanium oxynitride is an unexpected result given this intensive scrutiny. The reason for its discovery in this work is the use of combinatorial chemical vapor deposition. CVD provides a radically different reaction pathway compared to traditional solid-state techniques, and the combinatorial aspect involved allows a large number of conditions to be trialed simultaneously. This work, then, highlights the advantages that both a combinatorial approach and the use of nontraditional synthetic methods can present to materials research.

Conclusions

In this paper a new ternary oxynitride, $Ti_{3-\delta}O_4N$, with a range of titanium ion vacancy $\delta = 0.06-0.27$ has been described. The chemical composition was confirmed by XPS analysis and the structure of the $\delta = 0.15$ phase, $Ti_{2.85(2)}O_4N$, was determined from Rietveld refinement against powder X-ray diffraction data recorded using a synchrotron source. The compound was made using a combinatorial approach to CVD and shows how this approach may be a fruitful method for new phase synthesis. The novel oxynitride is isostructural to the high-temperature phase of Ti_3O_5, a preference for this *Cmcm* structure at room temperature similar to that frequently observed by cationic doping of Ti_3O_5, and caused in both cases by the removal of titanium d-electrons that are used in the room-temperature undoped Ti_3O_5 to form the metal−metal bonds that stabilize the monoclinic structure. The structural analysis of $Ti_{2.85(2)}O_4N$ shows that the nitrogen present substitutes for oxygen on a single crystallographic *4c* site. To our knowledge this is the first time that anionic doping has been carried out in the Ti_3O_5 structure and provides an interesting comparison to the extensive cationic doping studies carried out on the structure. Previous to this study the only binary titanium oxides known to incorporate nitrogen to form an oxynitride was the rock-salt TiO, and the very low levels of inclusion found in nitrogen-doped titania. This discovery of $Ti_{3-\delta}O_4N$ based on Ti_3O_5 opens up the possibility of forming many oxynitrides based on the range of binary oxides known for titanium.

Acknowledgment. The EPSRC is thanked for funding. Pilkington Group Limited is thanked for supplying glass substrates. For assistance with spectroscopic measurements we would like to thank Dr. Russell Binions, and for help with SEM measurements we thank Mr. Kevin Reeve. Dr. Larry Margulies, ESRF, is especially thanked for his generous assistance and efforts with the diffraction experiments. I.P.P. is a Wolfson/Royal Society merit award holder.

Supporting Information Available: UV−visible transmission spectra of the different colored sections of the films discussed; a full list of bond angles from the Rietveld refinement of $Ti_{3-\delta}O_4N$. This material is available free of charge via the Internet at http://pubs.acs.org.

JA073355S